

# 1 Reconstruction of solar UV irradiance since 1974

N. A. Krivova,<sup>1</sup> S. K. Solanki,<sup>1,2</sup> T. Wenzler,<sup>1,3</sup> and B. Podlipnik<sup>1</sup>

---

N. A. Krivova, Max-Planck-Institut für Sonnensystemforschung, Max-Planck-Str. 2, 37191  
Katlenburg-Lindau, Germany (natalie@mps.mpg.de)

S. K. Solanki, Max-Planck-Institut für Sonnensystemforschung, Max-Planck-Str. 2, 37191  
Katlenburg-Lindau, Germany

T. Wenzler, Hochschule für Technik Zürich, CH-8004 Zürich, Switzerland

B. Podlipnik, Max-Planck-Institut für Sonnensystemforschung, Max-Planck-Str. 2, 37191  
Katlenburg-Lindau, Germany

<sup>1</sup>Max-Planck-Institut für  
Sonnensystemforschung, D-37191  
Katlenburg-Lindau, Germany

<sup>2</sup>School of Space Research, Kyung Hee  
University, Yongin, Gyeonggi 446-701,  
Korea

<sup>3</sup>Hochschule für Technik Zürich, CH-8004  
Zürich, Switzerland

arXiv:0907.1500v1 [astro-ph.SR] 9 Jul 2009

**Abstract.**

Variations of the solar UV irradiance are an important driver of chemical and physical processes in the Earth's upper atmosphere and may also influence global climate. Here we reconstruct solar UV irradiance in the range 115–400 nm over the period 1974–2007 by making use of the recently developed empirical extension of the SATIRE models employing SUSIM data. The evolution of the solar photospheric magnetic flux, which is a central input to the model, is described by the magnetograms and continuum images recorded at the Kitt Peak National Solar Observatory between 1974 and 2003 and by the MDI instrument on SoHO since 1996. The reconstruction extends the available observational record by 1.5 solar cycles. The reconstructed Ly- $\alpha$  irradiance agrees well with the composite time series by *Woods et al.* [2000]. The amplitude of the irradiance variations grows with decreasing wavelength and in the wavelength regions of special interest for studies of the Earth's climate (Ly- $\alpha$  and oxygen absorption continuum and bands between 130 and 350 nm) is one to two orders of magnitude stronger than in the visible or if integrated over all wavelengths (total solar irradiance).

## 1. Introduction

19 Solar irradiance variations show a strong wavelength dependence. Whereas the total  
20 (integrated over all wavelengths) solar irradiance (TSI) changes by about 0.1% over the  
21 course of the solar cycle, the irradiance in the UV part of the solar spectrum varies by up  
22 to 10% in the 150–300 nm range and by more than 50% at shorter wavelengths, including  
23 the Ly- $\alpha$  emission line near 121.6 nm [e.g. *Floyd et al.*, 2003a]. On the whole, more than  
24 60% of the TSI variations over the solar cycle are produced at wavelengths below 400 nm  
25 [*Krivova et al.*, 2006; cf. *Harder et al.*, 2009].

26 These variations may have a significant impact on the Earth’s climate system. Ly- $\alpha$ ,  
27 the strongest line in the solar UV spectrum, which is formed in the transition region and  
28 the chromosphere, takes an active part in governing the chemistry of the Earth’s upper  
29 stratosphere and mesosphere, e.g., by ionizing nitric oxide, which affects the electron den-  
30 sity distribution, or by stimulating dissociation of water vapor and producing chemically  
31 active HO(x) that destroy ozone [e.g. *Frederick*, 1977; *Brasseur and Simon*, 1981; *Huang*  
32 *and Brasseur*, 1993; *Fleming et al.*, 1995; *Egorova et al.*, 2004; *Langematz et al.*, 2005a].  
33 Also, radiation in the Herzberg oxygen continuum (200–240 nm) and the Schumann-  
34 Runge bands of oxygen (180–200 nm) is important for photochemical ozone production  
35 [e.g. *Haigh*, 1994, 2007; *Egorova et al.*, 2004; *Langematz et al.*, 2005b; *Rozanov et al.*,  
36 2006; *Austin et al.*, 2008]. UV radiation in the wavelength range 200–350 nm, i.e. around  
37 the Herzberg oxygen continuum and the Hartley-Huggins ozone bands, is the main heat  
38 source in the stratosphere and mesosphere [*Haigh*, 1999, 2007; *Rozanov et al.*, 2004, 2006].

39 The record of regular measurements of the solar UV irradiance spectrum, accurate  
40 enough to assess its variations, goes back to 1991, when the Upper Atmosphere Research  
41 Satellite (UARS) was launched. Among others, it carried two instruments for monitor-  
42 ing solar radiation in the UV, the Solar Ultraviolet Spectral Irradiance Monitor [SUSIM;  
43 *Brueckner et al.*, 1993] and the Solar Stellar Irradiance Comparison Experiment [SOL-  
44 STICE; *Rottman et al.*, 1993]. These data sets are of inestimable value, but remain too  
45 short to allow reliable evaluation of solar influence on the Earth's climate and need to be  
46 extended back in time with the help of models.

47 Reconstructions of solar UV irradiance have earlier been presented by *Fligge and Solanki*  
48 [2000] and by *Lean* [2000]. The first one was based on LTE (Local Thermodynamic Equi-  
49 librium) calculations of the solar spectrum and the latter on UARS/SOLSTICE measure-  
50 ments. The LTE approximation gives inaccurate results below approximately 200 nm and  
51 in some spectral lines, whereas the long-term uncertainty of SOLSTICE (as well as of all  
52 other instruments that measured solar UV irradiance before SORCE) exceeded the solar  
53 cycle variation above approximately 250 nm, thus leading to incorrect estimates of the UV  
54 irradiance variability at longer wavelengths [see *Lean et al.*, 2005; *Krivova et al.*, 2006].

55 Whereas considerable advance has recently been made in modelling the variations of  
56 the total solar irradiance and the irradiance at wavelengths longer than about 300 nm  
57 [e.g., *Unruh et al.*, 1999; *Ermolli et al.*, 2003; *Krivova et al.*, 2003; *Wenzler et al.*,  
58 2004, 2005, 2006], models at shorter wavelengths have not kept apace. This is because  
59 the LTE approximation usually taken in calculations of the brightness of different pho-  
60 tospheric components fails in this wavelength range and non-LTE calculations are much  
61 more arduous [e.g. *Fontenla et al.*, 1999, 2006; *Haberreiter et al.*, 2005].

62 An alternative approach has been developed by *Krivova and Solanki* [2005a] and  
63 *Krivova et al.* [2006] that allows an empirical extrapolation of the successful SATIRE  
64 models [*Krivova and Solanki*, 2005b; *Solanki et al.*, 2005] down to 115 nm using avail-  
65 able SUSIM measurements. *Krivova et al.* [2006] have combined this technique with the  
66 model of *Krivova et al.* [2003] to reconstruct the variations of the solar UV irradiance over  
67 the period 1996–2002, i.e. the rising phase of cycle 23, using MDI (Michelson Doppler  
68 Imager on SoHO) [*Scherrer et al.*, 1995] magnetograms and continuum images. Here we  
69 employ the data from the National Solar Observatory Kitt Peak (NSO KP), in order to  
70 reconstruct the solar UV irradiance spectrum back to 1974. We then combine this KP-  
71 based reconstruction for the period 1974–2002 with the reconstruction based on MDI data  
72 [*Krivova et al.*, 2006], which has now been extended to 2006. In order to fill in the gaps in  
73 daily data and to extend the time series to 2007, when MDI continuum images displayed  
74 deteriorating quality, we employ the Mg II core-to-wing ratio and the solar F10.7 cm radio  
75 flux. Hence the present paper extends the work of *Krivova et al.* [2006] to three cycles,  
76 i.e. the whole period of time over which high quality magnetograms are available.

77 The model is described in Sect. 2, the results are presented in Sect. 3 and summarised  
78 in Sect. 4.

## 2. Model

79 We take a similar approach as *Krivova et al.* [2006]. This means that variations of  
80 the solar total and spectral irradiance on time scales of days to decades are assumed to  
81 be entirely due to the evolution of the solar surface magnetic field. Under this assump-  
82 tion, *Krivova et al.* [2003] and *Wenzler et al.* [2005, 2006] have successfully modelled the  
83 observed variations of the total solar irradiance. *Krivova et al.* [2006] showed that this

84 (SATIRE) model also works well in the spectral range 220–240 nm (hereinafter, the ref-  
85 erence range). They then analysed SUSIM data and worked out empirical relationships  
86 between the irradiance in this range and irradiances at all other wavelengths covered by  
87 the SUSIM detectors (115–410 nm). Thus if the irradiance in the range 220–240 nm is  
88 known, it is also possible to calculate irradiance at other wavelengths in the UV down to  
89 115 nm.

### 2.1. Solar irradiance at 220–240 nm

90 In a first step, we apply the SATIRE model [Spectral and Total Irradiance REconstruc-  
91 tions, *Solanki et al.*, 2005; *Krivova and Solanki*, 2008] to NSO KP magnetograms and  
92 continuum images, in order to reconstruct solar irradiance in the reference range for the  
93 period 1974–2003. In SATIRE, the solar photosphere is divided into 4 components: the  
94 quiet Sun, sunspot umbrae, sunspot penumbrae and bright magnetic features (describing  
95 both faculae and the network). Each component is described by the time-independent  
96 spectrum calculated from the corresponding model atmospheres in the LTE approxima-  
97 tion [*Unruh et al.*, 1999]. Since the distribution of the magnetic field on the solar surface  
98 evolves continuously, the area covered by each of the components on the visible solar  
99 disc also changes. This is represented by the corresponding filling factors, which are re-  
100 trieved from the magnetograms and continuum images. In the period 1974–2003, such  
101 data were recorded (nearly daily) with the 512-channel Diode Array Magnetograph [be-  
102 fore 1992; *Livingston et al.*, 1976] and the Spectromagnetograph [after 1992; *Jones et al.*,  
103 1992] on Kitt Peak [see also *Wenzler et al.*, 2006]. Since 1996 magnetograms and con-  
104 tinuum images were also recorded by the MDI instrument on SoHO. More details about

105 the SATIRE model have been given by *Fligge et al.* [2000]; *Krivova et al.* [2003]; *Wenzler*  
106 *et al.* [2005, 2006].

107 This model has one free parameter,  $B_{\text{sat}}$ , denoting the field strength below which the  
108 facular contrast is proportional to the magnetogram signal, while it is independent (sat-  
109 urated) above that. It depends on the quality (noise level and spatial resolution) of the  
110 employed magnetograms. From a comparison with the PMOD composite [*Fröhlich*, 2006]  
111 of the TSI measurements, *Wenzler et al.* [2006, 2009] found the value of  $B_{\text{sat}} = 320$  G for  
112 the KP data, whereas *Krivova et al.* [2003] obtained a value of  $B_{\text{sat}} = 280$  G for the MDI  
113 data. In this work we use the same values of this parameter and do not vary them any  
114 more in order to fit the spectral data.

115 The solar irradiance integrated over the wavelength range 220–240 nm reconstructed  
116 from the KP magnetograms and continuum images is shown in Fig. 1 by the red plus signs  
117 connected by the dashed line where there are no gaps in the daily sequence of data. The  
118 measurements by the SUSIM instrument are represented by the green line. We use daily  
119 level 3BS V22 data with a sampling of 1 nm (*Floyd et al.*, 2003b; L. Floyd, priv. comm.).  
120 A similar plot obtained with MDI data was given by *Krivova et al.* [2006]. The apparent  
121 change in the behavior between cycles 22 and 23 seen in Fig. 1a is due to the incorrect  
122 estimate of the degradation during the solar minimum period (L. Floyd, priv. comm.).  
123 This is, for example, confirmed by a comparison with the Mg II core-to-wing ratio, which  
124 is free of such problems, and is discussed in more detail by *Krivova et al.* [2006]. The fact  
125 that a single shift in absolute values applied to the SUSIM data before 1996 is sufficient in  
126 order to bring the data in agreement with the model also supports this conjecture. Indeed,  
127 in Fig. 1b the period before 1996 is shown on an enlarged scale. Here the measurements

128 by SUSIM were shifted in the absolute level by a fixed value ( $-5.0 \times 10^6 \text{ Wm}^{-3}\text{nm}$ ), and  
129 a good correspondence between the model and the data is seen.

130 This is also demonstrated by Fig. 2, where the measured irradiance at 220–240 nm  
131 is plotted against the modelled values. Dots and plus signs are used for the data from  
132 cycles 22 and 23, respectively (no correction to the absolute level has been applied). The  
133 dashed straight line with a slope of 0.95 represents the regression to all points. The  
134 correlation coefficient is 0.93. The solid line with a slope of 1.02 is the regression to the  
135 cycle 23 data only. It is hardly distinguishable from the thick dotted line with a slope of  
136 1.0 expected for a perfect fit. The corresponding correlation coefficient is 0.94, i.e. the  
137 same as found by *Wenzler et al.* [2006] for the modelled TSI compared to the PMOD  
138 composite for the period since 1992. We stress that the value of the free parameter,  $B_{\text{sat}}$ ,  
139 was the same in both cases. This means that SATIRE reproduces independent SUSIM  
140 data without any further adjustments, which is yet another success of the model.

141 In Fig. 1a, we also plot SOLSTICE data [*Woods et al.*, 1996] represented by the blue  
142 dashed line. Note that for comparison sake the SOLSTICE absolute values have been  
143 shifted by  $-4.3 \times 10^6 \text{ Wm}^{-3}\text{nm}$ . It is clear that at 220–240 nm the model is in a better  
144 agreement with the SUSIM data, even if the correction due to the degradation is not  
145 taken into account, than with the measurements by SOLSTICE, which also show a higher  
146 scatter.

147 Solar irradiance in the reference range for the period 1996–2002 was also reconstructed  
148 by *Krivova et al.* [2006] using MDI magnetograms and continuum images (Fig. 2 of that  
149 paper). We have updated their model through the beginning of 2006 and combined it  
150 with the KP-based reconstruction shown in Fig. 1. On the days when both models are

151 available, the preference was given to the MDI-based values, since they were found to be  
152 more accurate [cf. *Krivova et al.*, 2003; *Wenzler et al.*, 2004, 2006].

153 Unfortunately, the flat field distortion progressively affecting MDI continuum images  
154 requires a correction of all images recorded after approximately 2005 before they can be  
155 employed for the irradiance reconstructions. Such a correction is being attempted, but  
156 the outcome is not certain and it seems advisable to complete the reconstruction instead  
157 of waiting an unknown length of time.

158 There are also some gaps in the daily reconstructions, when no magnetograms and  
159 continuum images were recorded, in particular, in the 1970s. On the other hand, climate  
160 models often require solar signal input with a daily cadence. Therefore, we have employed  
161 the Mg II core-to-wing ratio [*Viereck et al.*, 2004] and the solar F10.7 cm radio flux [*Tanaka*  
162 *et al.*, 1973] in order to fill in the gaps and to extend the data to 2007. This has been done  
163 by using a linear regression between the irradiance in the reference range (220–240 nm)  
164 and the Mg II index (the linear correlation coefficient is  $R_c = 0.98$ ) and a quadratic  
165 relationship between the irradiance in the reference range and the F10.7 flux ( $R_c = 0.92$ ).  
166 Mg II and F10.7 cm flux data are obtained from the National Geophysical Data Center  
167 (NGDC; <http://www.ngdc.noaa.gov/ngdc.html>).

## 2.2. UV spectral irradiance

168 In order to extrapolate the SATIRE model based on KP NSO and MDI magnetograms  
169 and continuum images to other UV wavelengths, we made use of the relations between  
170 irradiances,  $F_\lambda$ , at a given wavelength,  $\lambda$ , and in the reference interval,  $F_{\text{ref}}$  (220–240 nm).  
171 These relationships in the range 115–410 nm were deduced by *Krivova et al.* [2006] using  
172 daily SUSIM data recorded between 1996 and 2002. We have repeated this analysis

173 with the data set extended to 2005, but did not find any significant difference to the  
174 earlier derived values and therefore employed the relationships from the previous work for  
175 consistency.

176 Using the calculated irradiances at 220–240 nm and empirical relationships  $F_\lambda/F_{\text{ref}}$  vs.  
177  $F_{\text{ref}}$ , solar UV irradiance at 115–270 nm was reconstructed for the whole period 1974–  
178 2007. Since the long term uncertainty of SUSIM measurements becomes comparable to  
179 or higher than the solar cycle variation at around 250 and 300 nm, respectively [*Woods*  
180 *et al.*, 1996; *Floyd et al.*, 2003b], above 270 nm SATIRE is found to be more accurate  
181 than the measurements [*Krivova et al.* 2006, cf. *Unruh et al.* 2008], Therefore spectral  
182 irradiance values at these wavelengths are calculated directly from SATIRE.

### 3. Results

#### 3.1. Ly- $\alpha$ irradiance

183 The Ly- $\alpha$  line is of particular interest not just for its prominence in the solar spectrum  
184 and its importance for the Earth’s upper atmosphere, but also because for this line a  
185 composite of measurements is available for the whole period considered here. In Fig. 3  
186 we compare the reconstructed solar Ly- $\alpha$  irradiance (red) with the composite time series  
187 (blue) compiled by *Woods et al.* [2000]. The latter record comprises the measurements  
188 from the Atmospheric Explorer E (AE-E, 1977–1980), the Solar Mesosphere Explorer  
189 (SME, 1981–1989), UARS SOLSTICE (1991–2001), and the Solar EUV Experiment (SEE)  
190 on TIMED (Thermosphere, Ionosphere, Mesosphere Energetics and Dynamic Mission  
191 launched in 2001). The gaps are filled in using proxy models based on Mg core-to-wing  
192 and F10.7 indices, and the F10.7 model is also used to extrapolate the data set back in  
193 time. The UARS SOLSTICE data are used as the reference, and other measurements

194 and the models are adjusted to the SOLSTICE absolute values. Although this time series  
195 is thus only partly based on direct Ly- $\alpha$  observations, it is the nearest we found to an  
196 observational time series to compare our model with.

197 For comparison, the SUSIM measurements are also plotted (green). The model agrees  
198 well with the SUSIM data, which confirms that our semi-empirical technique works well.  
199 Note that there is no change in the behavior around the minimum in 1996. This is yet  
200 another indication of the instrumental origin of the jump in the absolute values seen in  
201 SUSIM's irradiances at 220–240 and many other wavelengths [see *Krivova et al.*, 2006].

202 As Fig. 3 shows, there is some difference (about 5%) in the magnitude of the Ly-  
203  $\alpha$  solar cycle variations between SOLSTICE and SUSIM. Since our model agrees with  
204 SUSIM (by construction), a difference of this magnitude remains also between our model  
205 and SOLSTICE. Other than that, the model agrees with the completely independent  
206 composite time series very well, with a correlation coefficient of 0.95 (remember that  
207 the free parameter of the SATIRE model was fixed from a comparison with the PMOD  
208 composite of the TSI and not varied to fit the UV data).

209 The solar Ly- $\alpha$  irradiance has also been modelled by *Haberreiter et al.* [2005] using the  
210 filling factors derived from the MDI and KP NSO magnetograms and continuum images in  
211 combination with the brightness spectra for the quiet Sun, sunspots and faculae calculated  
212 with their NLTE code COSI. The calculated variability was about a factor of 2 lower than  
213 the measured one. NLTE calculation are, in principal, better suitable for calculations of  
214 the solar UV irradiance and they have recently made significant progress [e.g., *Fontenla*  
215 *et al.*, 2006, 2007; *Haberreiter et al.*, 2008]. Their complexity and the number of processes

216 to be accounted for do not, however, as yet allow an accurate reconstruction of the solar  
217 spectral irradiance over broader spectral ranges and longer periods of time.

### 3.2. Solar UV irradiance at 115–400 nm in 1974–2007

218 Figure 4 shows the reconstructed solar UV irradiance in the range 115–400 nm over  
219 the period 1974–2007 (i.e. covering cycles 21–23), normalized to the mean at each wave-  
220 lengths over the complete time period. At all considered wavelengths, the irradiance  
221 changes in phase with the solar cycle, in agreement with recent results based on 4 years  
222 of SIM/SORCE measurements [*Harder et al.*, 2009]. The variability becomes significantly  
223 stronger towards shorter wavelengths: from about 1% over the activity cycle at around  
224 300 nm to more than 100% in the vicinity of Ly- $\alpha$ .

225 Figure 5 shows the solar UV irradiance integrated over spectral ranges of particular  
226 interest for climate studies as a function of time: (a) 130–175 nm, (b) 175–200 nm, (c)  
227 200–242 nm, and (d) 200–350 nm. Solar radiation at 130–175 nm (Schumann-Runge  
228 continuum) is completely absorbed in the thermosphere. Over activity cycles 21–23, solar  
229 radiative flux in this spectral range varied by about 10–15% (Fig. 5a), i.e. by more  
230 than a factor of 100 more than solar cycle variations in the solar total energy flux (total  
231 solar irradiance). In the oxygen Schumann-Runge bands (175–200 nm) and Herzberg  
232 continuum (200–242 nm), important for photochemical ozone production and destruction  
233 in the stratosphere and mesosphere, solar irradiance varied on average by about 5–8%  
234 (Fig. 5b) and 3% (Fig. 5c), respectively. In the Hartley-Huggins ozone bands between  
235 200 and 350 nm, solar radiation is the main heat source in the stratosphere. At these  
236 wavelengths, the amplitude of the solar cycle variation is of the order of 1%, which is still  
237 an order of magnitude stronger than variations of the total solar irradiance.

238 The complete data set of the reconstructed solar irradiance at 115–400 nm over the pe-  
239 riod 1974–2007 is available as auxiliary material and under [http://www.mps.mpg.de/projects/sun-](http://www.mps.mpg.de/projects/sun-climate/data.html)  
240 [climate/data.html](http://www.mps.mpg.de/projects/sun-climate/data.html).

#### 4. Summary

241 *Krivova et al.* [2006] have developed an empirical technique, which allows an extrapo-  
242 lation of the magnetogram-based reconstructions of solar total and spectral irradiance to  
243 shorter wavelengths, down to 115 nm. They applied this technique to obtain variations  
244 of solar UV irradiance between 1996 and 2002. We have now extended their model to  
245 both earlier and more recent times. Thus we provide a reconstruction of the solar UV  
246 irradiance spectrum between 115 and 400 nm over the period 1974–2007. This extends the  
247 available observational record by about 1.5 solar cycles, i.e. roughly doubles the available  
248 record.

249 As a test of the quality of our model, we have compared the reconstructed solar Ly- $\alpha$   
250 irradiance with the completely independent composite of measurements and proxy models  
251 by *Woods et al.* [2000]. There is a small (about 5%) difference in the solar cycle amplitude  
252 between our model and that composite. This difference is also present between the SUSIM  
253 and SOLSTICE data, which are the reference sets for the model and the composite,  
254 respectively. Aside from that, the modelled and composite records closely agree with each  
255 other.

256 Solar UV irradiance varies in phase with the solar cycle at all wavelengths between  
257 115 and 400 nm, in agreement with the recent finding of *Harder et al.* [2009] based on  
258 SIM/SORCE measurements over 2004–2007. The relative amplitude of the variations  
259 grows with decreasing wavelength. In the wavelength regions important for studies of the

260 Earth's climate (e.g., Ly- $\alpha$  and oxygen absorption continuum and bands between 130 and  
261 350 nm), the relative variation is one to two orders of magnitude stronger than in the  
262 visible or if integrated over all wavelengths (i.e. TSI).

263 SATIRE-based reconstructed UV irradiance in the spectral range 115–400 nm between  
264 January 1, 1974 and December 31, 2007 is available as auxiliary material and under  
265 <http://www.mps.mpg.de/projects/sun-climate/data.html>.

266 **Acknowledgments.** We thank L. Floyd for providing SUSIM data and valuable com-  
267 ments and V. Holzwarth for helpful discussions. The composite Lyman  $\alpha$  time series was  
268 retrieved from the LASP ftp server ([laspftp.colorado.edu](http://laspftp.colorado.edu)). This work was supported by  
269 the Deutsche Forschungsgemeinschaft, DFG project number SO 711/2 and by the WCU  
270 grant No. R31-10016 funded by the Korean Ministry of Education, Science and Tech-  
271 nology. We also thank the International Space Science Institute (Bern) for giving us the  
272 opportunity to discuss this work with the great international team on “Interpretation and  
273 modelling of SSI measurements”.

## References

- 274 Austin, J., K. Tourpali, E. Rozanov et al. (2008), Coupled chemistry climate model  
275 simulations of the solar cycle in ozone and temperature, *J. Geophys. Res.*, *113*, doi:  
276 10.1029/2007JD009391.
- 277 Brasseur, G., and P. C. Simon (1981), Stratospheric chemical and thermal response to  
278 long-term variability in solar UV irradiance, *J. Geophys. Res.*, *86*, 7343–7362.
- 279 Brueckner, G. E., K. L. Edlow, L. E. Floyd, J. L. Lean, and M. E. Vanhoosier (1993), The  
280 solar ultraviolet spectral irradiance monitor (SUSIM) experiment on board the Upper

- 281 Atmosphere Research Satellite (UARS), *J. Geophys. Res.*, *98*(17), 10,695–10,711.
- 282 Egorova, T., E. Rozanov, E. Manzini, M. Haberreiter, W. Schmutz, V. Zubov, and T. Pe-  
283 ter (2004), Chemical and dynamical response to the 11-year variability of the solar  
284 irradiance simulated with a chemistry-climate model, *Geophys. Res. Lett.*, *31*, 6119–  
285 6122.
- 286 Ermolli, I., F. Berrilli, and A. Florio (2003), A measure of the network radiative properties  
287 over the solar activity cycle, *Astron. Astrophys.*, *412*, 857–864.
- 288 Fleming, E. L., S. Chandra, C. H. Jackman, D. B. Considine, and A. R. Douglass (1995),  
289 The middle atmospheric response to short and long term solar UV variations: analysis  
290 of observations and 2D model results, *J. Atmos. Terr. Phys.*, *57*, 333–365.
- 291 Fligge, M., and S. K. Solanki (2000), The solar spectral irradiance since 1700, *Geophys.*  
292 *Res. Lett.*, *27*, 2157–2160.
- 293 Fligge, M., S. K. Solanki, and Y. C. Unruh (2000), Modelling irradiance variations from  
294 the surface distribution of the solar magnetic field, *Astron. Astrophys.*, *353*, 380–388.
- 295 Floyd, L., G. Rottman, M. DeLand, and J. Pap (2003a), 11 years of solar UV irradiance  
296 measurements from UARS, *ESA SP*, *535*, 195–203.
- 297 Floyd, L. E., J. W. Cook, L. C. Herring, and P. C. Crane (2003b), SUSIM'S 11-year  
298 observational record of the solar UV irradiance, *Adv. Space Res.*, *31*, 2111–2120.
- 299 Fontenla, J., O. R. White, P. A. Fox, E. H. Avrett, and R. L. Kurucz (1999), Calculation  
300 of solar irradiances. I. Synthesis of the solar spectrum, *Astrophys. J.*, *518*, 480–499.
- 301 Fontenla, J. M., E. Avrett, G. Thuillier, and J. Harder (2006), Semiempirical Models of the  
302 Solar Atmosphere. I. The Quiet- and Active Sun Photosphere at Moderate Resolution,  
303 *Astrophys. J.*, *639*, 441–458.

- 304 Fontenla, J. M., K. S. Balasubramaniam, and J. Harder (2007), Semiempirical Models of  
305 the Solar Atmosphere. II. The Quiet-Sun Low Chromosphere at Moderate Resolution,  
306 *Astrophys. J.*, *667*, 1243–1257.
- 307 Frederick, J. E. (1977), Chemical response of the middle atmosphere to changes in the  
308 ultraviolet solar flux, *Planet. Space Sci.*, *25*, 1–4.
- 309 Fröhlich, C. (2006), Solar irradiance variability since 1978: Revision of the PMOD com-  
310 posite during solar cycle 21, *Space Sci. Rev.*, *125*, 53–65.
- 311 Haberreiter, M., N. A. Krivova, W. Schmutz, and T. Wenzler (2005), Reconstruction of  
312 the solar UV irradiance back to 1974, *Adv. Space Res.*, *35*, 365–369.
- 313 Haberreiter, M., W. Schmutz, and I. Hubeny (2008), NLTE model calculations for the  
314 solar atmosphere with an iterative treatment of opacity distribution functions, *Astron.*  
315 *Astrophys.*, *492*, 833–840.
- 316 Haigh, J. D. (1994), The role of stratospheric ozone in modulating the solar radiative  
317 forcing of climate, *Nature*, *370*, 544–546.
- 318 Haigh, J. D. (1999), Modelling the impact of solar variability on climate, *J. Atm. Terr.*  
319 *Phys.*, *61*, 63–72.
- 320 Haigh, J. D. (2007), The Sun and the Earth’s Climate, *Liv. Rev. Sol. Phys.*,  
321 <http://solarphysics.livingreviews.org/Articles/lrsp-2007-2/>.
- 322 Harder, J. W., J. M. Fontenla, P. Pilewskie, E. C. Richard, and T. N. Woods (2009),  
323 Trends in solar spectral irradiance variability in the visible and infrared, *Geophys. Res.*  
324 *Lett.*, *36*, doi:10.1029/2008GL036797.
- 325 Huang, T. Y. W., and G. P. Brasseur (1993), Effect of long-term solar variability in  
326 a two-dimensional interactive model of the middle atmosphere, *J. Geophys. Res.*, *98*,

- 327 20,413–20,428.
- 328 Jones, H. P., T. L. Duvall, J. W. Harvey, C. T. Mahaffey, J. D. Schwitters, and J. E.  
329 Simmons (1992), The NASA/NSO spectromagnetograph, *Solar Phys.*, *139*, 211–232.
- 330 Krivova, N. A., and S. K. Solanki (2005a), Reconstruction of solar UV irradiance, *Adv.*  
331 *Space Res.*, *35*, 361–364.
- 332 Krivova, N. A., and S. K. Solanki (2005b), Modelling of irradiance variations through  
333 atmosphere models, *Mem. Soc. Astron. It.*, *76*, 834–841.
- 334 Krivova, N. A., and S. K. Solanki (2008), Models of solar irradiance variations: Current  
335 status, *J. Astroph. Astron.*, *29*, 151–158.
- 336 Krivova, N. A., S. K. Solanki, M. Fligge, and Y. C. Unruh (2003), Reconstruction of  
337 solar total and spectral irradiance variations in cycle 23: is solar surface magnetism the  
338 cause?, *Astron. Astrophys.*, *399*, L1–L4.
- 339 Krivova, N. A., S. K. Solanki, and L. Floyd (2006), Reconstruction of solar UV irradiance  
340 in cycle 23, *Astron. Astrophys.*, *452*, 631–639.
- 341 Langematz, U., J. L. Grenfell, K. Matthes, P. Mieth, M. Kunze, B. Steil, and C. Brühl  
342 (2005a), Chemical effects in 11-year solar cycle simulations with the Freie Universität  
343 Berlin Climate Middle Atmosphere Model with online chemistry (FUB-CMAM-CHEM),  
344 *Geophys. Res. Lett.*, *32*, 13,803, doi:10.1029/2005GL022686.
- 345 Langematz, U., K. Matthes, and J. L. Grenfell (2005b), Solar impact on climate: modeling  
346 the coupling between the middle and the lower atmosphere, *Mem. Soc. Astron. It.*, *76*,  
347 868–875.
- 348 Lean, J. (2000), Evolution of the Sun’s Spectral Irradiance Since the Maunder Minimum,  
349 *Geophys. Res. Lett.*, *27*, 2425–2428, doi:10.1029/2000GL000043.

- 350 Lean, J., G. Rottman, J. Harder, and G. Kopp (2005), SORCE Contributions to New  
351 Understanding of Global Change and Solar Variability, *Solar Phys.*, *230*, 27–53, doi:  
352 10.1007/s11207-005-1527-2.
- 353 Livingston, W. C., J. Harvey, C. Slaughter, and D. Trumbo (1976), Solar magnetograph  
354 employing integrated diode arrays, *Appl. Opt.*, *15*, 40–52.
- 355 Rottman, G. J., T. N. Woods, and T. P. Sparn (1993), Solar-Stellar Irradiance Comparison  
356 Experiment. I - Instrument design and operation, *J. Geophys. Res.*, *98 (D6)*, 10,667–  
357 10,677.
- 358 Rozanov, E., T. Egorova, W. Schmutz, and T. Peter (2006), Simulation of the strato-  
359 spheric ozone and temperature response to the solar irradiance variability during sun  
360 rotation cycle, *J. Atm. Sol.-Terr. Phys.*, *68*, 2203–2213.
- 361 Rozanov, E. V., M. E. Schlesinger, T. A. Egorova, B. Li, N. Andronova, and V. A.  
362 Zubov (2004), Atmospheric response to the observed increase of solar UV radia-  
363 tion from solar minimum to solar maximum simulated by the University of Illi-  
364 nois at Urbana-Champaign climate-chemistry model, *J. Geophys. Res.*, *109 (D1)*,  
365 doi:10.1029/2003JD003,796.
- 366 Scherrer, P. H., et al. (1995), The Solar Oscillations Investigation - Michelson Doppler  
367 Imager, *Solar Phys.*, *162*, 129–188.
- 368 Solanki, S. K., N. A. Krivova, and T. Wenzler (2005), Irradiance models, *Adv. Space Res.*,  
369 *35*, 376–383.
- 370 Tanaka, H., J. P. Castelli, A. E. Covington, A. Krüger, T. L. Landecker, and A. Tlamicha  
371 (1973), Absolute Calibration of Solar Radio Flux Density in the Microwave Region,  
372 *Solar Phys.*, *29*, 243–262.

- 373 Unruh, Y. C., S. K. Solanki, and M. Fligge (1999), The spectral dependence of facular  
374 contrast and solar irradiance variations, *Astron. Astrophys.*, *345*, 635–642.
- 375 Unruh, Y. C., N. A. Krivova, S. K. Solanki, J. W. Harder, and G. Kopp (2008), Spectral  
376 irradiance variations: comparison between observations and the SATIRE model on solar  
377 rotation time scales, *Astron. Astrophys.*, *486*, 311–323.
- 378 Viereck, R. A., L. E. Floyd, P. C. Crane, T. N. Woods, B. G. Knapp, G. Rottman,  
379 M. Weber, L. C. Puga, and M. T. DeLand (2004), A composite Mg II index spanning  
380 from 1978 to 2003, *Space Weather*, *2*, doi:10.1029/2004SW000084.
- 381 Wenzler, T., S. K. Solanki, N. A. Krivova, and D. M. Fluri (2004), Comparison between  
382 KPVT/SPM and SoHO/MDI magnetograms with an application to solar irradiance  
383 reconstructions, *Astron. Astrophys.*, *427*, 1031–1043.
- 384 Wenzler, T., S. K. Solanki, and N. A. Krivova (2005), Can surface magnetic fields repro-  
385 duce solar irradiance variations in cycles 22 and 23?, *Astron. Astrophys.*, *432*, 1057–1061.
- 386 Wenzler, T., S. K. Solanki, N. A. Krivova, and C. Fröhlich (2006), Reconstruction of  
387 solar irradiance variations in cycles 21–23 based on surface magnetic fields, *Astron.*  
388 *Astrophys.*, *460*, 583–595.
- 389 Wenzler, T., S. K. Solanki, and N. A. Krivova (2009), Reconstructed and measured total  
390 solar irradiance: Is there a secular trend between 1978 and 2003?, *Geophys. Res. Lett.*,  
391 *36*, L11102, doi:10.1029/2009GL037519.
- 392 Woods, T. N., D. K. Prinz, G. J. Rottman et al. (1996), Validation of the UARS solar  
393 ultraviolet irradiances: Comparison with the ATLAS 1 and 2 measurements, *J. Geophys.*  
394 *Res.*, *101 (D6)*, 9541–9570.
- 395 Woods, T. N., W. K. Tobiska, G. J. Rottman, and J. R. Worden (2000), Improved solar

- 396 Lyman- $\alpha$  irradiance modeling from 1947 through 1999 based on UARS observations, *J.*  
397 *Geophys. Res.*, *105*(A12), 27,195–27,215.

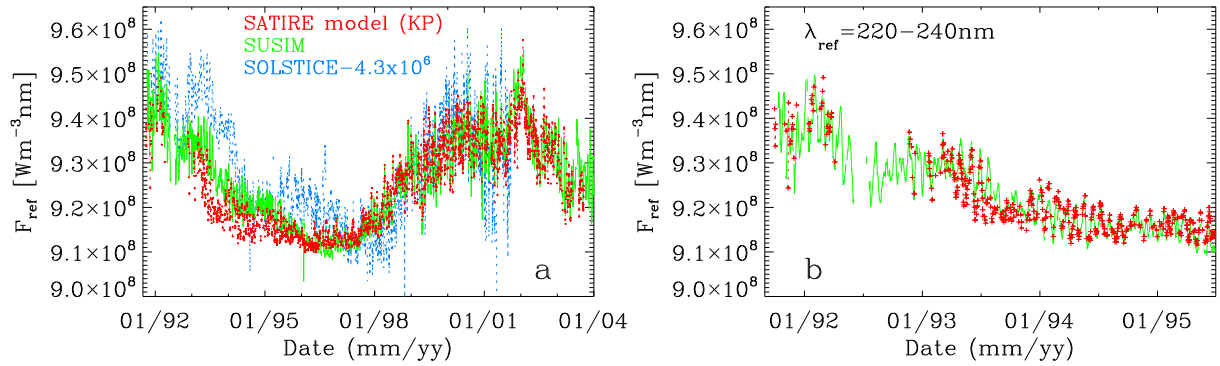


**Figure 1.** (a) The solar irradiance integrated over the wavelength range 220–240 nm as a function of time for the period 1991–2003. The green line shows SUSIM measurements [Floyd *et al.*, 2003b] and the red plus signs (connected by the dashed line where there are no gaps) the values reconstructed using SATIRE models and KP magnetograms. SOLSTICE data [Woods *et al.*, 1996] shifted by  $-4.3 \times 10^6 \text{Wm}^{-3}\text{nm}$  are shown by the blue dashed line. (b) Enlargement of the panel a restricted to the period before 1996 showing only SUSIM data and the reconstruction. Here SUSIM data were shifted by  $-5.0 \times 10^6 \text{Wm}^{-3}\text{nm}$ .

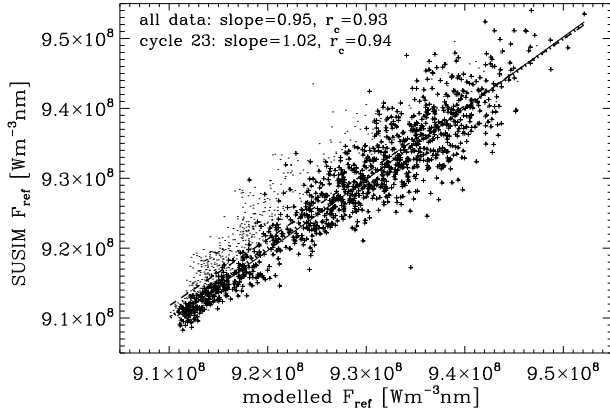


**Figure 2.** The solar irradiance in the range 220–240 nm: as measured by SUSIM vs. reconstructed by SATIRE. Dots and pluses are used for cycles 22 and 23, respectively. The dashed straight line is the regression to all points (with no correction applied to SUSIM’s absolute level). The solid line is the regression for cycle 23 only. The thick dotted line almost coinciding with the solid line shows the expectation value, i.e. a slope of 1.0 and no offset. Correlation coefficients and slopes are indicated in the figure.

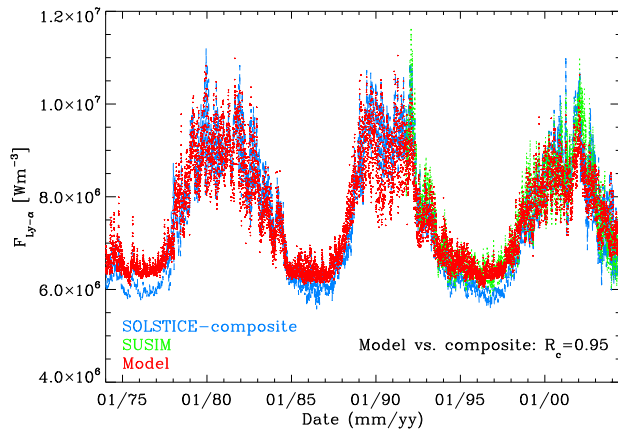


**Figure 3.** Solar Ly- $\alpha$  irradiance since 1974: reconstructed by SATIRE (red), measured by the SUSIM instrument (green) and compiled by *Woods et al.* [2000, blue].

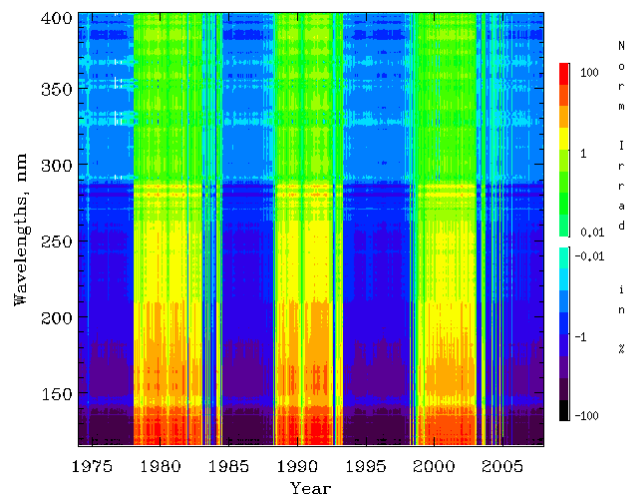


**Figure 4.** The reconstructed solar UV irradiance at 115–400 nm in the period 1974–2007 normalized to the mean at each wavelength over the whole period of time.

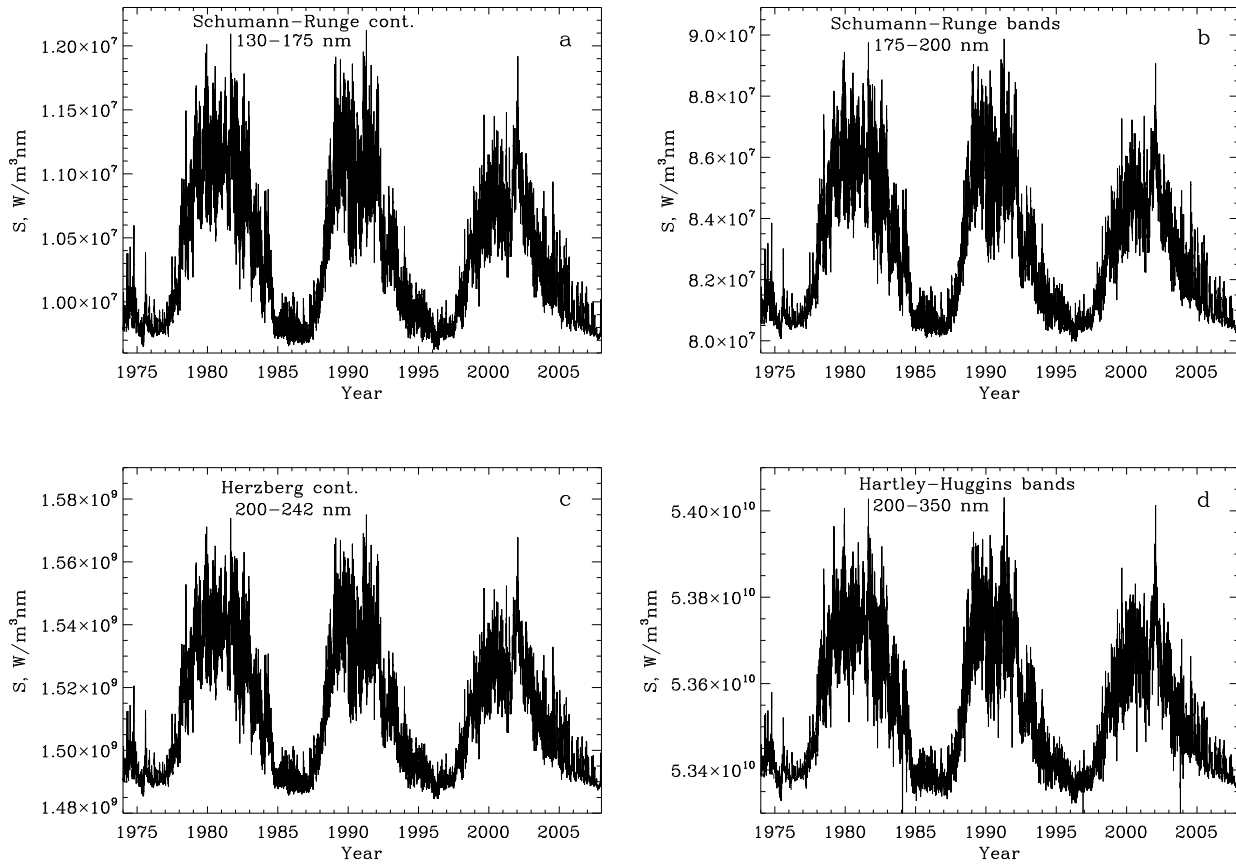


**Figure 5.** Reconstructed solar irradiance in the period 1974–2007 integrated over the wavelength ranges: (a) 130–175 nm (Schumann-Runge continuum), (b) 175–200 nm (Schumann-Runge bands), (c) 200–242 nm (Herzberg continuum), and (d) 200–350 nm (Hartley-Huggins bands).